Nanometer-Scale Ion Aggregates in Aqueous Electrolyte Solutions: Guanidinium Sulfate and Guanidinium Thiocyanate

P. E. Mason,[†] C. E. Dempsey,[§] G. W. Neilson,[‡] and J. W. Brady*,[†]

Department of Food Science, Stocking Hall, Cornell University, Ithaca, New York 14853; H.H. Wills Physics Laboratory, University of Bristol, Bristol BS8 1TL, UK; and Department of Biochemistry, University of Bristol, Bristol BS8 1TD, UK

Received: May 26, 2005; In Final Form: October 24, 2005

Neutron diffraction experiments and molecular dynamics simulations are used to study the structure of aqueous solutions of two electrolytes: guanidinium sulfate (a mild protein conformation stabilizer) and guanidinium thiocyanate (a powerful denaturant). The MD simulations find the unexpected result that in the Gdm_2SO_4 solution the ions aggregated into mesoscopic (nanometer-scale) clusters, while no such aggregation is found in the GdmSCN solution. The neutron diffraction studies, the most direct experimental probe of solution structure, provide corroborating evidence that the predicted very strong ion pairing does occur in solutions of 1.5 *m* Gdm_2SO_4 but not in 3 *m* solutions of GdmSCN. A mechanism is proposed as to how this mesoscopic solution structure affects solution denaturant properties and suggests an explanation for the Hofmeister ordering of these solutions in terms of this ion pairing and the ability of sulfate to reverse the denaturant power of guanidinium.

The structure of electrolyte solutions is an important subject in both fundamental and practical chemistry but has long been controversial due to the lack of experimental data. Many salts readily dissolve in water as they replace the ionic interactions of their crystal lattices with ion−dipole interactions to multiple water molecules. These ion−water interactions are very strong, and the coordinated water molecules are so highly structured that their resulting entropy change is generally unfavorable, typically exceeding even that for solvating hydrophobic species.[1] The degree of correlation between like and oppositely charged ions in a salt solution has, however, proven difficult to characterize experimentally. The solvated ions may be randomly distributed in solution or may exhibit residual associational structure. Perhaps most interesting are the suggestions that like-charged ions might form spatially correlated pairs in aqueous solution due to the special structuring imposed on the solvent water. Recently, it has been proposed that such pairing might occur for molecular ions like guanidinium[2−4] and could play an important role in such solution properties as the Hofmeister ranking of the ions.

Almost 120 years ago, Hofmeister ordered the common ions into series according to their effects on protein solubility and conformational stability.[5] This ranking for monatomic cations correlates with surface charge density, but for complex polyatomic ions, the underlying mechanisms for the Hofmeister series are less apparent.[6] For example, the guanidinium cation is an effective protein denaturant, while among anions, thiocyanate is a strong denaturant, chloride is essentially "neutral", and sulfate stabilizes proteins. It has long been common to attribute the differing effects of ions on proteins to changes which they were thought to induce in the collective structure of liquid water, with some ions being described as "structure makers", or kosmotropes, and others being characterized as "structure breakers", or chaotropes. Recent studies have not necessarily supported this simple picture.[6−9] Solutes clearly structure those water molecules with which they directly interact in their hydration shells,[7,10,11] but the effects on more distant bulk water molecules appear to be less significant.[8] The interactions of molecular ions with water are expected to be much more complex than for atomic ions, and the differences in the effects of these ions on the solubility and conformational stability of proteins may need explanations which are specific for each molecular species.

Recently we reported the use of molecular dynamics (MD) simulations to interpret neutron diffraction with isotopic substitution (NDIS) experiments on the intermolecular structuring in aqueous solutions of guanidinium chloride.[4] The measured neutron diffraction is a direct function of the structure of the solution, while the simulations allow qualitative interpretations of the scattering data in terms of that solution structuring.[12] The studies found a rich variety of ionic structuring in GdmCl, including a tendency for the guanidinium ions to stack in a parallel manner. The present paper describes the use of similar NDIS experiments and MD simulations to characterize aqueous solutions of guanidinium thiocyanate and guanidinium sulfate. These new studies find very different collective structuring in these two solutions and yield experimental evidence for ion pairing which is confirmed by modeling and indicate how the natures of the different counterions for guanidinium give rise to their Hofmeister ranking. For the guanidinium sulfate case the ionic association was found to produce extended aggregates on the nanometer size scale.

Methods

Experimental Procedures. Neutron scattering patterns were obtained from the D4C diffractometer at the Institut Laue-Langevin, Grenoble, for solutions containing 1.50 mol of Gdm_2-

[†] Cornell University.
[‡] H.H. Wills Physics Laboratory, University of Bristol.
[§] Department of Biochemistry, University of Bristol.
* To whom correspondence should be addressed.

10.1021/jp052799c CCC: $30.25
Published on Web 11/24/2005

SO_4 and 3.00 mol of GdmSCN per 55.55 mol of water (and hereafter referred to as 1.5 M* Gdm_2SO_4 and 3.0 M* GdmSCN) in H_2O, D_2O, and HDO. These solutions were prepared by direct dissolution of the salts in water (both solutions having identical concentrations of Gdm^+). The scattering patterns were corrected for multiple scattering, incoherent scattering, and absorption and were normalized to a standard vanadium rod to give the $F(Q)$ of the isotopically labeled solution. $F(Q)$ can be written as

$$F(Q) = \sum_{\alpha}\sum_{\beta} c_\alpha c_\beta b_\alpha b_\beta (S_\alpha\beta(Q) - 1)$$

where c_α is the atomic concentration of species α whose neutron coherent scattering length is b_α, and the sums are over all five atomic species in the solution, which in order of concentration are H, O, N, C, and S. $S_{\alpha\beta}(Q)$ is the partial structure factor of atoms α and β and is directly related to the radial pair distribution function $g_{\alpha\beta}(r)$ through Fourier transformation

$$g_{\alpha\beta}(r) - 1 = \frac{1}{2\pi^2\rho r}\int dQ(S_{\alpha\beta}(Q) - 1)Q \sin(Qr) \quad (1)$$

To underline the complexity of the solution, we note that $F(Q)$ contains 15 terms. However, because the coefficients $c_\alpha c_\beta b_\alpha b_\beta$ scale with the product of concentrations and the amplitude of the b's are roughly similar, the scattering patterns are dominated principally by correlations between hydrogen atoms themselves and to a progressively lesser degree between hydrogen and oxygen atoms and the other atoms in the two solutions. As we show below, by taking various differences among the three isotope-dependent $F(Q)$'s, it is possible to investigate at atomic resolution perturbations in the water structure due to the presence of the two ionic salts.

The method used to extract the atomic details of the solution is similar to that used in Mason et al.[7] The procedure used allows a determination of the pair distribution function $g_{HH}(r)$ and of ${}^nG_H{}^Y(r)$ and ${}^nG_Y{}^Y(r)$, each of which involve different linear combinations of the weighted pair radial distribution functions of the solution. As we show explicitly below, the dominant terms in ${}^nG_H{}^Y(r)$ and ${}^nG_Y{}^Y(r)$ are $g_{OH}(r)$ and $g_{OO}(r)$, respectively.

While there are many different nuclei present in these systems (O_w, O_{sulf}, S, H_w, H_{gdm}, N, and C for the Gdm_2SO_4 solution and O_w, S, C_{thio}, N_{thio}, H_w, H_{gdm}, N_{gdm}, and C_{gdm} for the GdmSCN solution), the neutrons are scattered by the atomic nucleus and so do not distinguish between chemically different atomic sites containing the same element. For simplicity, we only describe the NDIS measurements by element, although in later discussion the results are interpreted using structure factors of these chemically different nuclei as calculated from MD (which of course has the intrinsic ability to distinguish between atom types).

In the first instance $S_{HH}(Q)$ is calculated from the three $F(Q)$'s of each solution. The corresponding $g_{HH}(r)$'s of these solutions were calculated in a self-consistent way by Fourier transformation of $S_{HH}(Q)$ and analyzed to give information on the coordination of one hydrogen atom to its neighboring hydrogen atoms.

Subsequently, two additional partial structure functions are generated. The first of these, ${}^n\Delta_H{}^Y(Q)$, is obtained by subtraction of a suitably scaled $S_{HH}(Q)$ from the difference between the $F(Q)$'s of the heavy water and light water samples of each solution. This new function provides information associated with correlations between hydrogen atoms and all other atom types other than hydrogen and can be written as

$${}^n\Delta_H{}^Y(Q) = \frac{AS_{HO}(Q) + BS_{HN}(Q) + CS_{HC}(Q) + DS_{HS}(Q)}{A + B + C + D} - 1 \quad (2)$$

The superscript Y is used to represent a sum over non-hydrogen atom species. The superscript n indicates that this function is dimensionless, having been normalized by division by the sum of scattering prefactors, in this case A + B + C + D. The prefactors themselves are composed of a product of $c_\alpha c_\beta b_a \Delta b_H$, where $\Delta b_H = b_D - b_H$.

The Fourier transform of this function, ${}^nG_H{}^Y(r)$, provides information on the pairwise structural correlations between hydrogen atoms and all atoms other than hydrogen in the system. Specifically

$${}^nG_H{}^Y(r) = \frac{Ag_{HO}(r) + Bg_{HN}(r) + Cg_{HC}(r) + Dg_{HS}(r)}{A + B + C + D} - 1 \quad (3)$$

For the 1.5 M* Gdm_2SO_4 and 3.0 M* GdmSCN, the ${}^nG_H{}^Y(r)$'s were calculated to be respectively

$${}^nG_H{}^Y(r) = 0.767g_{OH}(r) + 0.181g_{NH}(r) + 0.042g_{CH}(r) + 0.009g_{SH}(r) - 1 \quad (4a)$$

and

$${}^nG_H{}^Y(r) = 0.667g_{OH}(r) + 0.232g_{NH}(r) + 0.083g_{CH}(r) + 0.018g_{SH}(r) - 1 \quad (4b)$$

The second partial structure−function, ${}^n\Delta_Y{}^Y(Q)$, is obtained by subtraction of a sum of suitably scaled $S_{HH}(Q)$ and ${}^n\Delta_H{}^Y(Q)$ from the heavy water total structure factor of each isotopically labeled solution. This function can be written as

$${}^n\Delta_Y{}^Y(Q) = ES_{OO}(Q) + FS_{ON}(Q) + GS_{OC}(Q) + HS_{NN}(Q) + IS_{OS}(Q) + JS_{NC}(Q) + KS_{CC}(Q) + LS_{CS}(Q) + MS_{NS}(Q) + NS_{SS}(Q)/[E + F + G + H + I + J + K + L + M + N] - 1$$

Fourier transformation of this function gives a radial distribution function, which contains pairwise correlations between all atoms other than hydrogen

$${}^nG_Y{}^Y(r) = Eg_{OO}(Qr) + Fg_{ON}(r) + Gg_{OC}(r) + Hg_{NN}(r) + Ig_{OS}(r) + Jg_{NC}(r) + Kg_{CC}(r) + Lg_{CS}(r) + Mg_{NS}(r) + Ng_{SS}(r)/[E + F + G + H + I + J + K + L + M + N] - 1 \quad (5)$$

For the 1.5 M* Gdm_2SO_4 and 3.0 M* GdmSCN, the ${}^nG_Y{}^Y(r)$'s were calculated to be respectively

$${}^nG_Y{}^Y(r) \cong 0.589g_{OO}(r) + 0.277g_{NO}(r) + 0.066g_{CO}(r) + 0.032g_{NN}(r) - 1 \quad (6a)$$

and

$${}^nG_Y{}^Y(r) \cong 0.445g_{OO}(r) + 0.310g_{NO}(r) + 0.110g_{CO}(r) + 0.054g_{NN}(r) - 1 \quad (6b)$$

where we have neglected the other six pair distribution functions

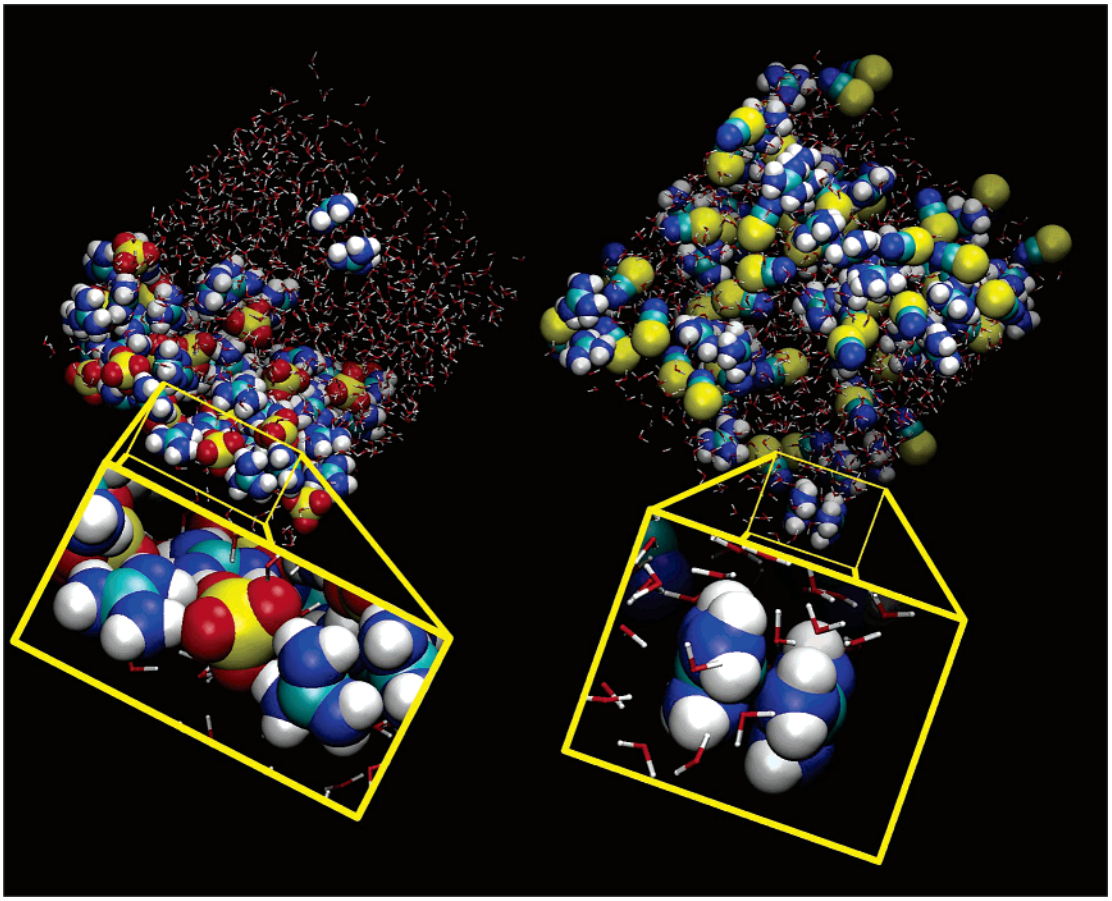

Figure 1. Snapshots of the Gdm_2SO_4 (left) and GdmSCN (right) simulations, shown using the molecular graphics program VMD.[41] In the Gdm_2SO_4 the ions aggregate strongly such that there are very few unpaired ions. In the GdmSCN solution the ions are much more homogeneously distributed. In each case one of the more common ion pairing motifs is shown.

($g_{CC}(r)$, $g_{CN}(r)$, $g_{CS}(r)$, $g_{NS}(r)$, $g_{OS}(r)$, $g_{SS}(r)$) as together they contribute less than 10% to the ${}^{n}G_{Y}^{Y}(r)$'s.

Computational Procedures. Simulations employed the CHARMM program,[13] with the TIP3P water[14,15] model and the same guanidinium force field used in our previous studies of guanidinium chloride.[4] Sulfate and thiocyanate were modeled using literature potentials[16,17] (sulfate atom charges: S, 2.4; O, −1.1; thiocyanate atom charges: N, −0.737; C, 0.483; S, −0.747). Arbitrary starting coordinates were generated by randomly placing and orienting 48 guanidinium and 48 SCN^- ions in a cubic box with sides of 34 Å superimposed on 1296 water molecules, and those waters which overlapped any solute heavy atoms were discarded. By design this procedure produced a 3 *m* solution (48 GdmSCN in 884 TIP3P water molecules, 3.02 M*). The box length was then rescaled to 32.3506 Å to yield the correct physical number density, 0.0968 atoms $Å^{-3}$. The sulfate simulations were set up in a similar manner (24 Gdm_2SO_4, 888 TIP3P waters, 1.50 M*, number density 0.102 $Å^{-3}$). Simulations were performed at 300 K following procedures used previously.[4] In those studies, the sensitivity to water model, guanidinium force field, and treatment of long-range interactions were tested, and the results were found to be qualitatively insensitive to these parameters. Here, following 5 ps of dynamics during which velocities were reassigned every 0.1 ps, the thiocyanate trajectory was integrated for 0.8 ns, with the first 0.3 ns excluded from analysis as an equilibration period. The guanidinium sulfate trajectory, which exhibited a slow relaxation process that required a longer time to complete, was integrated for 3.5 ns, with the first 1.5 ns of the simulation taken as equilibration. To test whether the aggregation observed in the guanidinium sulfate simulation was an artifact of initial conditions or simulation size (see discussion below), the temperature of the final frame of the simulation was subsequently randomly reassigned to 1200 K for 500 ps in order to disrupt the aggregates and then cooled again to 300 K in a single step by random reassignment of the atomic velocities at the lower temperature, followed by an additional 2 ns of dynamics. In addition, a similar box containing only 16 guanidinium ions and 8 sulfate anions in 888 water molecules, for a concentration of 0.50 M*, was simulated for 2 ns at 300 K using the procedures described for the 1.5 M* case.

Results and Discussion

MD Simulations. As shall be seen, both the NDIS experiments and the MD simulations found significant ion pairing in these aqueous solutions. In the simulations, both hetero-ion pairing and homo-ion pairing between the guanidinium ions were observed, as is shown in Figure 1. While in the simulations the guanidinium−thiocyanate pairs tended to be randomly distributed throughout the solution volume, the guanidinium−sulfate pairs exhibited a pronounced propensity to aggregate, which eventually resulted in a nanometer-scale mesoscopic ionic association of the system, similar to that observed in methanol/water mixtures,[18] or in the hydrophobic separation found in MD studies of methane in water.[19,20] However, the mode of aggregation in the present case is not like hydrophobic association, where the intermediate scale structure is driven toward minimizing the surface area. Here the ions tend to form dynamic wormlike chains about 1 nm in diameter or plates with

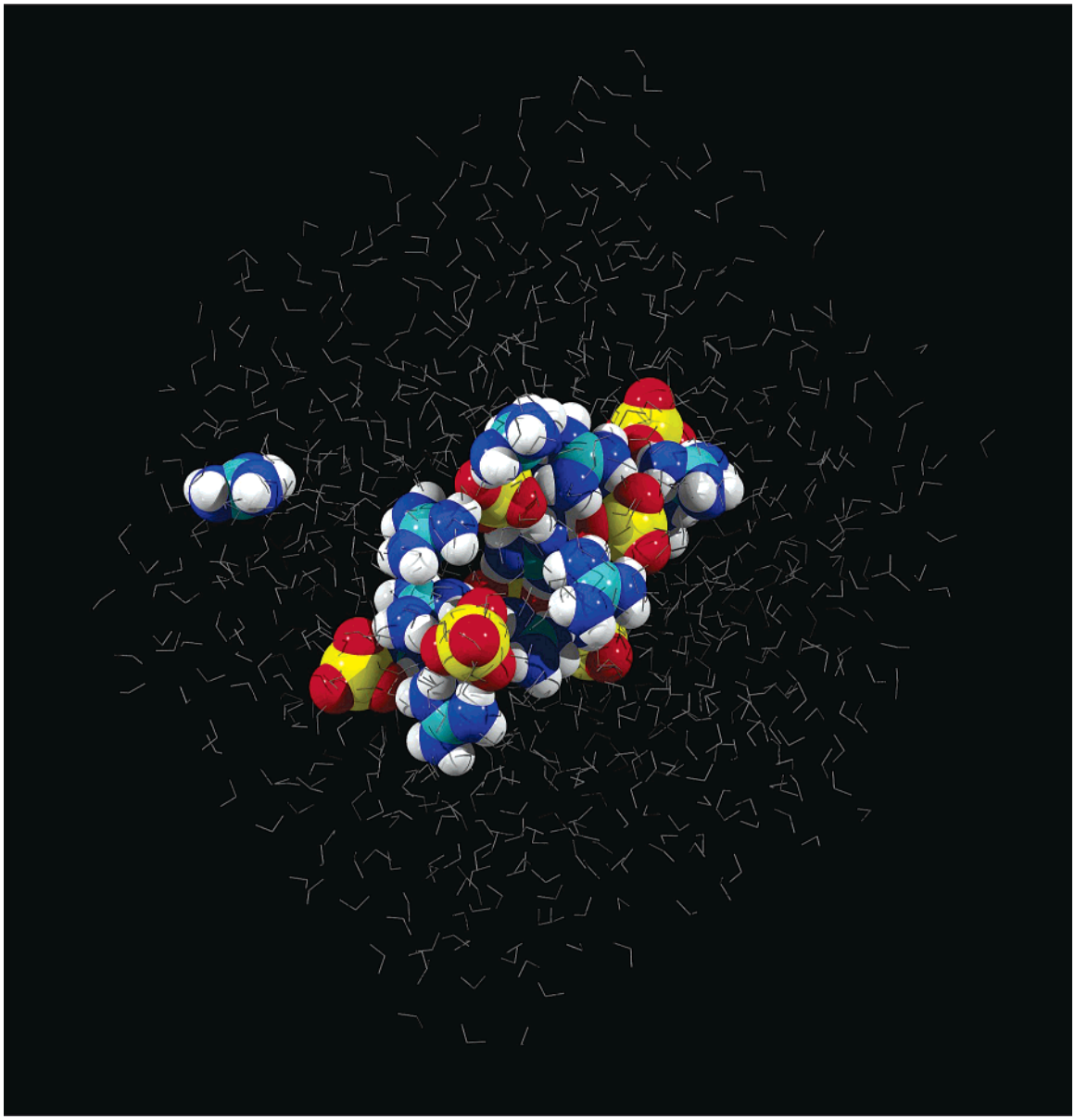

Figure 2. Snapshot of the last frame of the Gdm_2SO_4 simulation at 0.50 M*, showing that the aggregate forms at lower concentrations and is not an artifact of the periodic boundary conditions since in this case the aggregate does not span the length of the box.

dimensions comparable to the length of the box used in this simulation. The thickness of these aggregates is such that all ions are still in contact with the surrounding water molecules (i.e., there is no significant interior). This behavior distinguishes the clustering from an incipient phase separation, since in that case there would be a tendency for the cluster to become more spherical, creating an interior consisting of the new phase segregated from the aqueous medium. The structuring evident in Figure 1 is illustrated in more detail in a movie in the Supporting Information.

To determine whether the observed clustering might be a simulation artifact, several tests were carried out. In the first of these, the sulfate solution simulation was repeated at the lower concentration of 0.50 M*. The overall box size and density remained approximately the same, but in this new simulation, in which there were only 16 Gdm ions, there were not enough ions to form a cluster which would span the box and be repeated by the boundary condition symmetry. As can be seen in Figure 2, an aggregate again formed which involved essentially all of the ions but which was not periodic in the sense of being continuous with its images. This test demonstrated that the clustering tendency is not an artifact of the periodicity of the system and is not concentration dependent in this range. In another test, the final coordinates for the guanidinium sulfate simulation, which included the ionic aggregate, were heated to a temperature of 1200 K, whereupon the aggregate dispersed but spontaneously re-formed again upon cooling back to 300 K, showing that the aggregation was not an artifact of the initial conditions selection. In all three cases, the formation of the aggregates was relatively slow, requiring times of ~1 ns. To test the dependence of the observed aggregation on the atomic partial charges, another simulation was conducted in which the sulfate polarity was much lower, with oxygen charges of −0.5 and sulfur charges of 0.0; again aggregation was observed for the ions as before. Finally, the possibility of dependence on water model was investigated, since a previous study found that ion pairing can be significantly affected by the choice of water model.[21] A simulation setup in the same fashion as the first, with identical solute force field parameters, but using the SPC/E water model[22] was performed. This simulation exhibited the same clustering behavior as did the TIP3P simulation, indicating that the clustering is not an artifact of the water model.

While such aggregation has been observed previously in MD simulations of systems known from experiment to undergo phase separation[19,20] and while the present results are supported by experimental data as well, as shall be seen, it remains possible that the aggregation is favored by an entropy of mixing contribution to the total free energy which is too small due to the microscopic size of the system. Because of the already large size of these systems in computational terms, it is not practical to repeat the simulations with substantially larger boxes. However, the present simulation boxes are much larger than those used in previous studies which, in agreement with experiment, found aggregation.[19,20] It should also be noted that while the model Gdm_2SO_4 and GdmSCN systems are the same size, aggregation was repeatedly observed in the Gdm_2SO_4 case, but not in the GdmSCN solution. The reason that the mixing entropy term is probably not a concern in the present case is the very strong nature of the guanidinium−sulfate binding (see below). Since the binding is so strong, it was not possible to calculate the binding free energy from the simulations, since no stable dispersed state persisted long enough for meaningful averaging, as the aggregation began developing even during the equilibration phase. Given the very large enthalpy term from ion pairing favoring aggregation, the unfavorable entropy of mixing term is outweighed, and apparently this is so even in a macroscopic-sized sample.

The difference in the collective structure of these two solutions apparently results from the substantial qualitative differences in the direct hydrogen bonding of the anions to the common cation. The inter-proton cis **H**NCN**H** distance in the guanidinium ion and the **O**S**O** distance of the sulfate are very similar. The symmetric tetrahedral distribution of hydrogen-bonding acceptor oxygen atoms in the sulfate ion allows it to simultaneously form double hydrogen bonds with several guanidinium ions (hydrogen-bonding of these ions is topologically unfrustrated). Because of the nearly ideal linear geometry of these hydrogen bonds and the fact that both groups participating in these interactions are charged, the energies of these hydrogen bonds are higher than conventional hydrogen bonds or even hydrogen bonds between either ion and water.[23] These hydrogen bonds are of course also stronger than those in the thiocyanate case due to the higher charge of the sulfate ion. As a result, the sulfate ions form a dynamic network bridging between guanidinium molecules (Figure 1) and incorporating enough water molecules to satisfy the remaining hydrogen bonding capacity of the sulfate oxygen atoms. Despite the strength of these ion pair interactions, the ions still exchange places, although the lifetime of a heteroion pair is long (on the order of several tenths of a nanosecond).

To further characterize the solution structure, probability density maps were generated from the simulations for the distribution of water, other guanidinium ions, and counterions around the guanidinium ions (Figure 3). The exceptionally strong binding between the SO_4^{2-} and the Gdm^+ ions is evident in the distribution map for the sulfates around guanidinium. The highest of these contours is 50 times the average number density of sulfate oxygen atoms, which contrasts sharply with the GdmSCN simulation. This strong interaction of the SO_4^{2-} with the Gdm^+ is the driving force that determines the structuring of the solution.

The ordering of guanidinium ions around other guanidinium ions is significantly different in the two solutions. In the SO_4^{2-} solution there is much more Gdm^+-Gdm^+ ordering at an intermediate range (due to $Gdms^+$ held together by bridging SO_4^{2-} ions), while in the SCN solution, the Gdm^+-Gdm^+ ordering is weaker but is of a much more interesting stacking character, similar to that expected for hydrophobic, planar aromatic rings. We have observed such Gdm stacking previously in MD simulations of GdmCl solutions.[4] Interestingly, density maps for Gdm^+ correlations in 3 M* GdmCl are very similar to those in 3 M* GdmSCN (both solutions being powerful denaturants).

This difference in pairing behavior may be the significant factor in determining the Hofmeister ranking of these ions. Previously we related the hydrophobic-like hydration of the faces of the Gdm^+ ion, as indicated by the orientation of water around these faces and the propensity for the ions to stack in a hydrophobic fashion, to its denaturant properties.[4,24] In this model, the Gdm^+ ion can favorably interact at a molecular level with both hydrophobic and hydrophilic groups, augmenting protein solubility (salting in), destabilizing the folded native form, and promoting denaturation, while still interacting favorably with water via hydrogen bonds in the molecular plane.[4] The simulation results for the SO_4^{2-} solution are consistent with this interpretation, since the geometry of the strong aggregation of the Gdm^+ and SO_4^{2-} ions prevents hydrophobic hydration of the Gdm^+ faces, and by tying them up in the aggregation network makes them unavailable to bind to protein hydrophobic side chains. These observations support the theory that such denaturants function not though the modification of the bulk water structure, but by direct interaction with the protein itself, as has also been suggested for urea.[25]

Neutron Scattering Results. The results of the NDIS experiments support the modeling results, as appropriate corresponding signatures were observed in the experimental data of both the Gdm_2SO_4 and GdmSCN solutions to validate the MD calculations. Figure 4 presents the directly measured experimental difference functions ${}^n\Delta_Y{}^Y(Q)$ for both solutions and the residual that results from taking their difference. The MD results for these functions are also shown, as this is the purest form of comparison between MD and structural data that can be performed. To interpret the comparison between the MD and NDIS data in *Q*-space, it is necessary to recall some general features about the relationship between *Q*-space and *r*-space data. The intermolecular correlations, which are sharp features at relatively low r (>2.7 Å) in ${}^nG_Y{}^Y(r)$, are manifested in ${}^n\Delta_Y{}^Y(Q)$ as relatively lightly damped sine-like functions with a period of greater than about 2 $Å^{-1}$ and demonstrably constitute most of the signal above ca. 7 $Å^{-1}$. It should further be noted that the MD prediction shows oscillations in ${}^n\Delta_Y{}^Y(Q)$ above 16.5 $Å^{-1}$ (the experimental limit of D4C using a neutron wavelength of 0.7 Å). This means that the experimental structure obtained for the intermolecular correlations will be somewhat resolution-limited. Longer range structure is manifested by much more severely damped, higher frequency oscillations in $S(Q)$ (which have been essentially reduced to zero by 5 $Å^{-1}$), although this is convoluted by molecular correlations that also have significant frequency components in this range. The larger the *r*-space structure that is represented, the more severe the damping, and the higher the frequency of the oscillations in $S(Q)$.

If the experimental ${}^n\Delta_Y{}^Y(Q)$ is compared for Gdm_2SO_4 and GdmSCN, it is found that both structures at first sight are strikingly similar. The same is true for the MD data. However, the most pertinent examination of these data comes from the subtraction of ${}^n\Delta_Y{}^Y(Q)$ for the Gdm_2SO_4 and GdmSCN solutions (Figure 4c). For both the MD and NDIS data this difference function is very similar, most importantly in the region below 5 $Å^{-1}$. This fact demonstrates that while MD may only give a reasonable fit to the total structure of aqueous solutions, it is

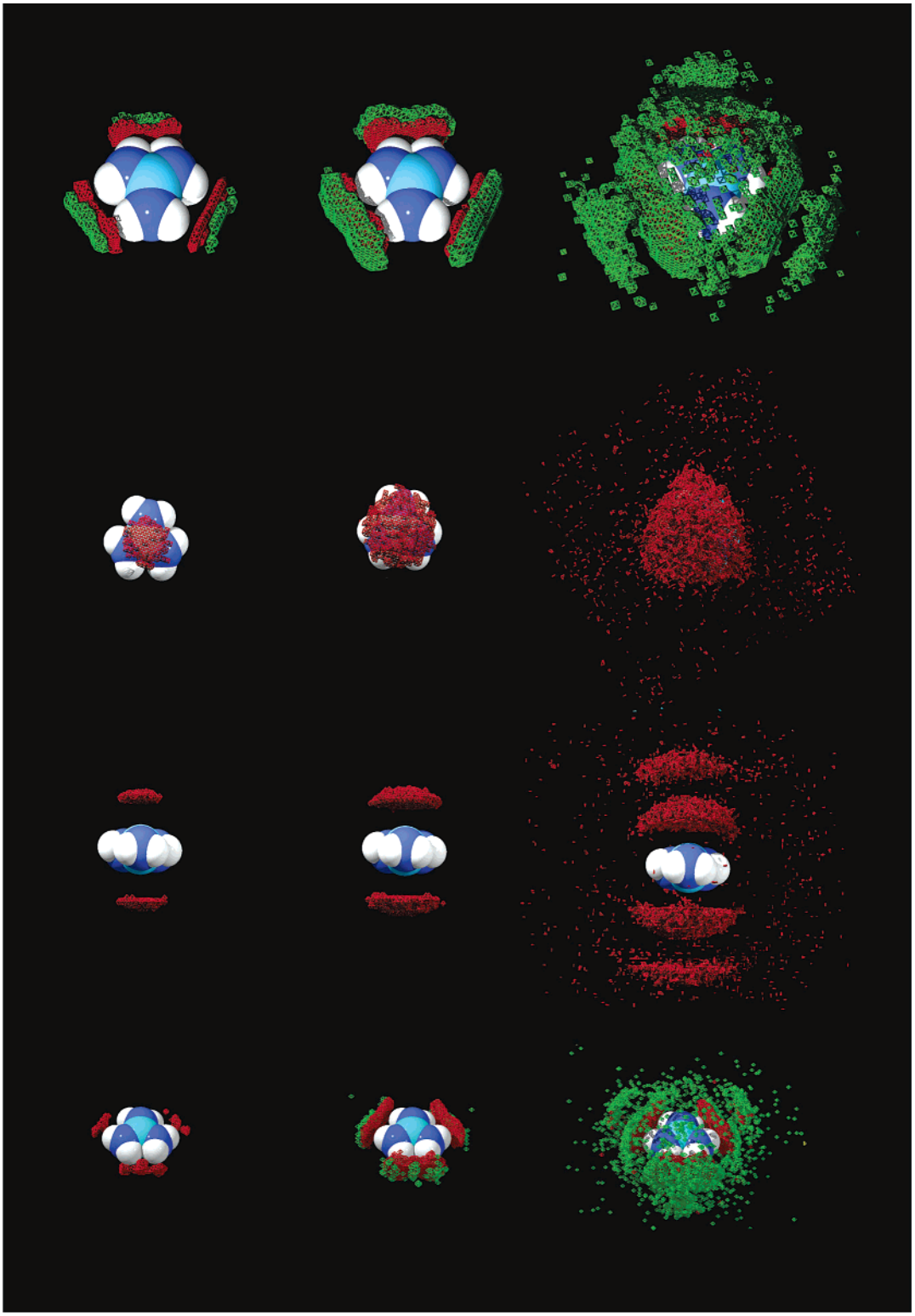

Figure 3. (a) Density maps, calculated using specifically developed software, for the species around the Gdm^+ ion as averaged from MD simulation of 3.0 M* GdmSCN solution (left). All density contour levels are given from left to right. Upper: the coordination of H and O around the Gdm ion; O contours (red) are shown at 9.26, 5.19, and 2.96 times the average number density of O (equal to 2.69, 1.51, and 0.86 times bulk number density); H(water) contours (green) are shown at 4.98, 2.78, and 1.59 times the average number density of H(water) (equal to 2.69, 1.51, and 0.86 times bulk number density). Upper middle and lower middle: the density maps of C(Gdm^+) around Gdm^+ (red) seen from "above" and from the plane of the Gdm^+ ion; Contours are at 11.24, 5.62, and 2.21 times the average number density of C(Gdm^+) (corresponding to 0.16, 0.083, and 0.032 times bulk number density). Bottom: the density maps of N(SCN^-) and S around Gdm^+. Contours for both N(SCN^-) (red) and S (green) are at 20, 7, and 4 times number density of each atom (corresponding to 0.29, 0.10, and 0.058 times bulk number density).

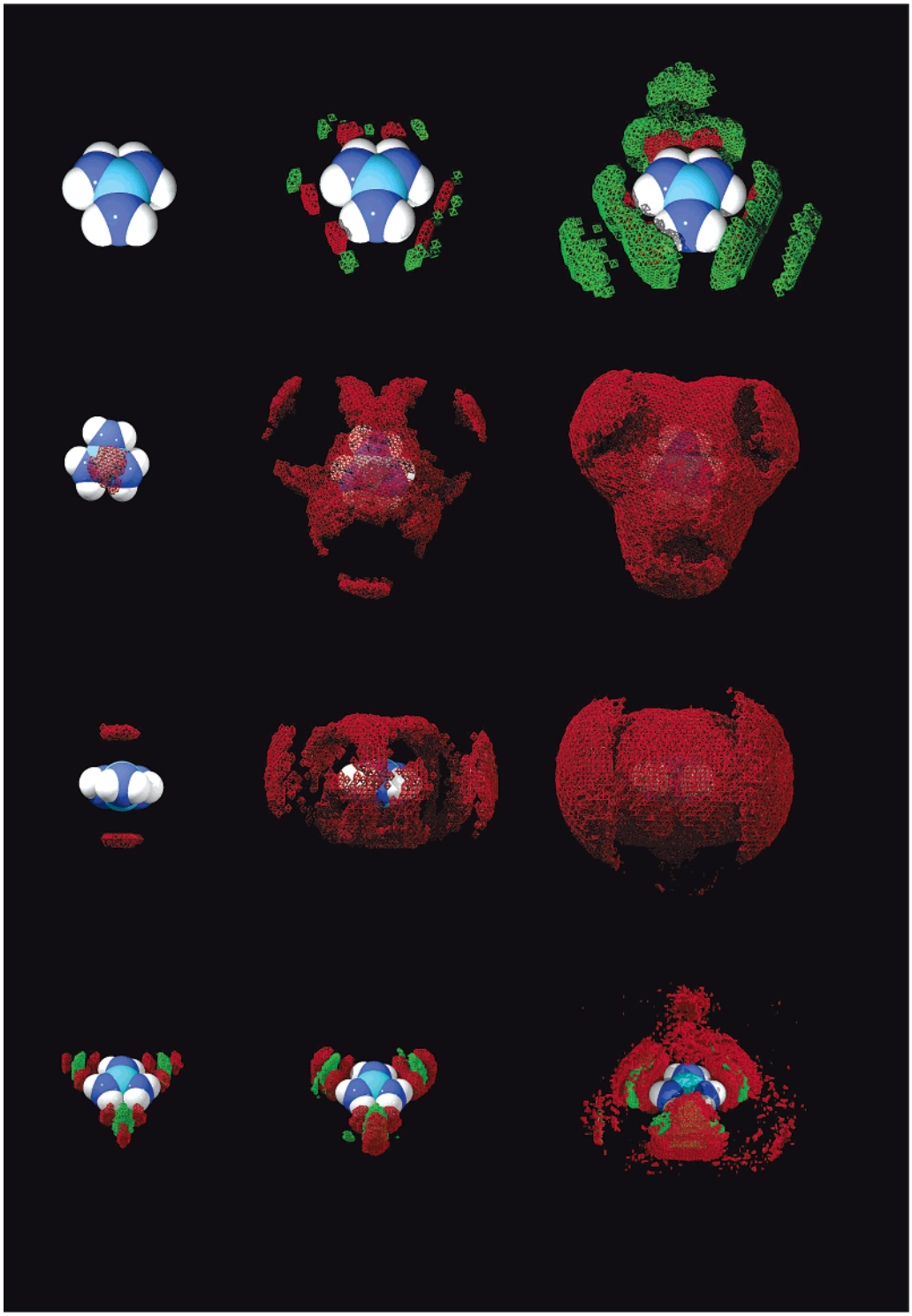

(b) Density maps for the species around the Gdm^+ ion as calculated from MD simulation of 1.5 M* Gdm_2SO_4 solution (right). All density contour levels are given from left to right. Upper: the coordination of H and O around the Gdm ion. O contours (red) are shown at 9.88, 5.55, and 3.16 times the average number density of O (equal to 2.69, 1.51, and 0.86 times bulk number density); H(water) contours (green) are shown at 4.71, 2.65, and 1.51 times the average number density of H(water) (equal to 2.69, 1.51, and 0.86 times bulk number density). Upper middle and lower middle: the density maps of C around Gdm^+ (red). Contours are at 11.24, 5.62, and 2.21 times the average number density of C (corresponding to 0.16, 0.083, and 0.032 times bulk number density). Bottom: the density maps of S (green) and O(sulfate) (red) around Gdm^+. Contours for both S and O(sulfate) are at 50, 15, and 2.5 times number density of each atom (corresponding to 1.47, 0.44, and 0.074 times bulk number density for O(sulfate) and 0.37, 0.11, and 0.019 times bulk number density for S). From the comparison of the bulk number density of O(sulfate) and O(water) around the Gdm^+ ion it is apparent that there are comparable populations of these two atom types H bonded to the Gdm^+ ion (despite the fact that there are 10 times more O(water) in this solution than O(sulfate)).

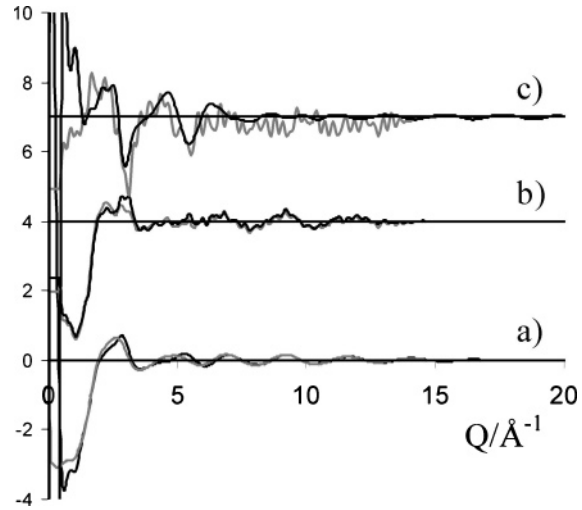

Figure 4. (a, b) ${}^{n}\Delta_{Y}{}^{Y}(Q)$, black line 1.5 *m* Gdm_2SO_4, gray line 3 *m* GdmSCN. (a) From MD. (b) From NDIS experiment. (c) The residue from ${}^{n}\Delta_{Y}{}^{Y}(Q)$, scaled by a factor of 7, for 1.5 *m* Gdm_2SO_4 subtracted from that for 3 *m* GdmSCN: black line, MD; gray line, NDIS.

very powerful at reproducing trends in these systems. This correspondence demonstrates that the principal difference between these two solutions (over the Q range studied here) is in the intermediate r-range, 4−7 Å.

The Fourier transforms of the structure factors allow the interpretation of the observed scattering in terms of actual structure in the solutions. From the correlation functions produced by this method it can be seen that the principal characteristics of the solution structure predicted by the simulations for the two different guanidinium counterions were observed directly in the neutron diffraction experiments. The most striking feature of the experimental functions $g_{HH}(r)$, ${}^{n}G_{H}{}^{Y}(r)$, and ${}^{n}G_{Y}{}^{Y}(r)$, shown in Figures 5 and 6, is that they are very similar for both Gdm_2SO_4 and GdmSCN. The similarity of $g_{HH}(r)$ and ${}^{n}G_{H}{}^{Y}(r)$ for both solutions, which is found in both the NDIS and MD results, does not support the theory that denaturants function through alteration of the water structure.

The function ${}^{n}G_{H}{}^{Y}(r)$ is composed of four radial distribution functions, $g_{HwOw}(r)$, $g_{HN}(r)$, $g_{HC}(r)$, and $g_{HS}(r)$. As shown below, the prefactor for the last of these is so small that this term can be safely ignored. In each case the very strong intramolecular peak corresponding to the HO bond has been removed from the data using literature procedures[7] in order to avoid Fourier transform artifacts from this very sharp and strong correlation. ${}^{n}G_{H}{}^{Y}(r)$ as determined from NDIS is shown in Figure 5 along with ${}^{n}G_{H}{}^{Y}(r)$ calculated from MD for both the Gdm_2SO_4 and GdmSCN solution. With the exception of the resolution-limited peak at 1.9 Å the ${}^{n}G_{H}{}^{Y}(r)$ calculated from MD is in good agreement with the NDIS experiment. Although it is not presently possible to directly resolve the experimental ${}^{n}G_{H}{}^{Y}(r)$ into its four component functions, this is possible with the simulation functions. The function $g_{HwOw}(r)$ calculated from MD (Figure 7) contributes at least two-thirds of the structure−function ${}^{n}G_{H}{}^{Y}(r)$ and is essentially the same for both the Gdm_2SO_4 solution and the GdmSCN solution.

While $g_{HwOw}(r)$ reflects the hydrogen bonding in aqueous solutions, the general structure is better defined by $g_{OwOw}(r)$. It has been shown that the second O−O peak at 4.5 Å in $g_{OwOw}(r)$ responds to both pressure and the presence of electrolytes in solution.[26] The $g_{OwOw}(r)$'s for the Gdm_2SO_4 and GdmSCN solutions also show only minor differences in the MD functions with no conspicuous signatures (Figure 7). However, it should be recalled that the TIP3P water model has only a

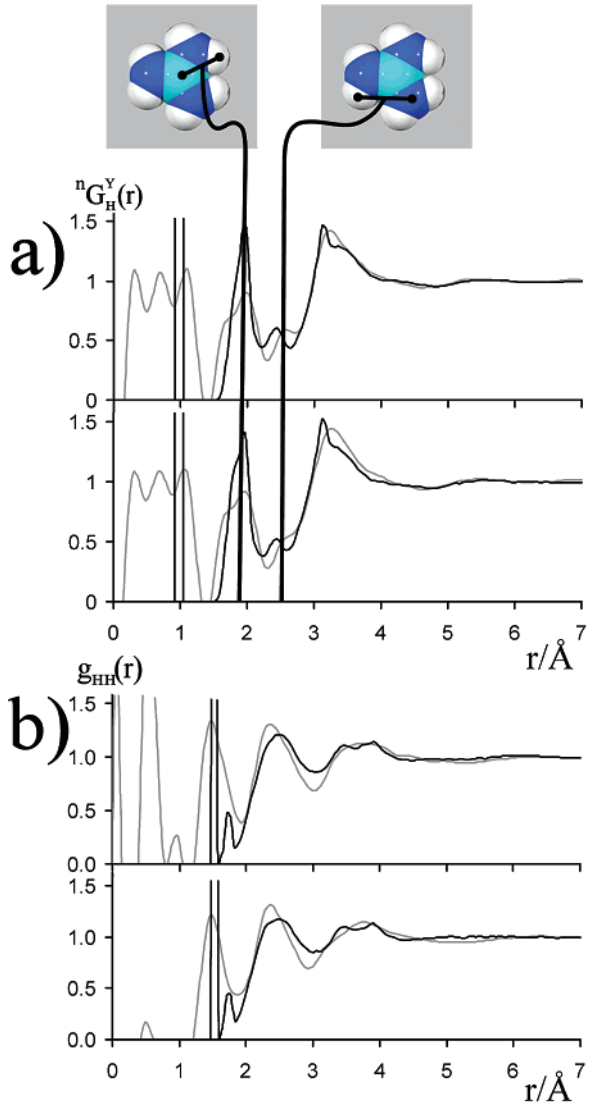

Figure 5. For each radial distribution function the MD simulation is shown as a black line and the NDIS result shown as a gray line. (a) ${}^{n}G_{H}{}^{Y}(r)$, (b) $g_{HH}(r)$. For both (a) and (b) the upper plot represents the GdmSCN solution; lower figure represents data concerning the Gdm_2SO_4 solution. Upon the ${}^{n}G_{H}{}^{Y}(r)$ plots the intramolecular Gdm^{+} correlations are highlighted. The principal reason for the difference in the sharpness of the peaks in the NDIS and MD results is that the NDIS results are significantly resolution limited for the sharper peaks.

weak second peak at 4.5 in $g_{OwOw}(r)$, yet this does not prevent the MD from successfully reproducing the signature for strong ion pairing. These observations suggest that it is not the "water structure" that is important in determining the denaturant power of a solution, but rather the direct interaction of the ions with the protein. This conclusion can be made with some confidence since, of the two solutions sharing similar water structure, one (GdmSCN) is the strongest of the guanidinium denaturant salts, while the other (Gdm_2SO_4) is weakly stabilizing of protein structure.

The experimental heavy atom correlation function ${}^{n}G_{Y}{}^{Y}(r)$ is the most complicated of the distributions determined here, but it is also the most useful and contains clear information to confirm the MD finding that very strong hetero-ion pairing occurs in Gdm_2SO_4 but not in GdmSCN. The function ${}^{n}G_{Y}{}^{Y}(r)$ (Figure 6) contains contributions from 10 $g(r)$'s; however, significant contributions are made only from $g_{OO}(r)$, $g_{ON}(r)$, and $g_{OC}(r)$ (see eq 6). Figure 6 compares this experimental correlation function for both solutions to the corresponding MD

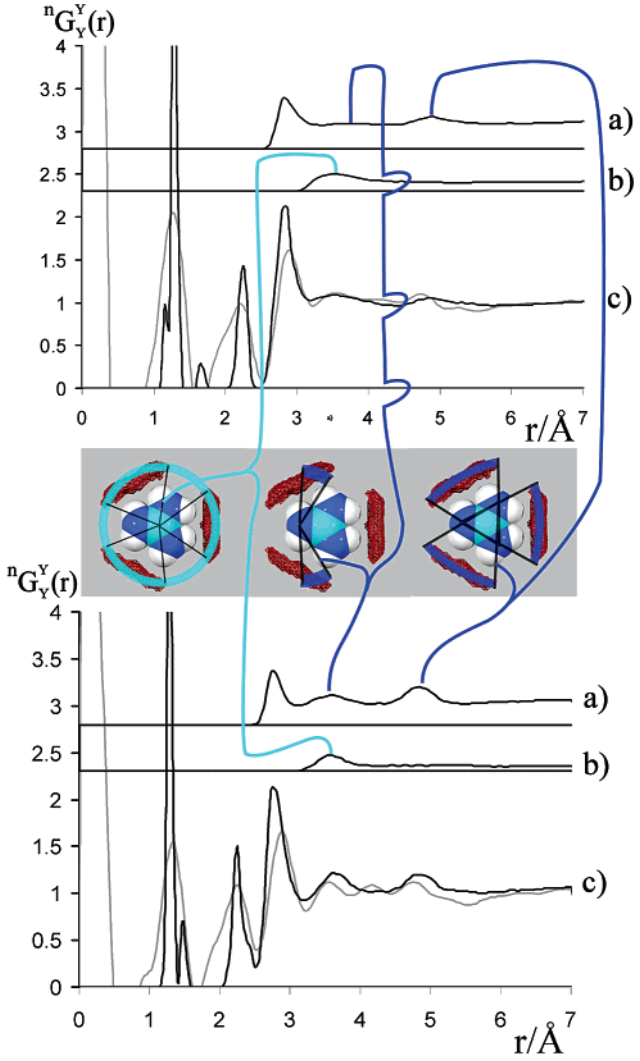

Figure 6. ${}^nG_Y{}^Y(r)$. Upper figure represents information about the GdmSCN solution; lower figure represents data concerning the Gdm_2SO_4 solution. Both figures have identical format. Lower gray line, ${}^nG_Y{}^Y(r)$ as determined by NDIS; black line, ${}^nG_Y{}^Y(r)$ as calculated from MD. Middle, the component of ${}^nG_Y{}^Y(r)$ due to $g_{OC}(r)$; upper, the component of ${}^nG_Y{}^Y(r)$ due to the $g_{ON}(r)$ correlation. Highlighted are the OC and ON intermolecular correlations (visible in the NDIS data) that relate directly to the hydration of the Gdm^+ ion. These are more pronounced in the Gdm_2SO_4 solution as the dominant mode of Gdm−O interaction is via ion pairing with the sulfate ion, which is considerably stronger than the Gdm−water interaction. This is direct structural evidence of very strong ion pairing of the Gdm^+ and SO_4^{2-} ion.

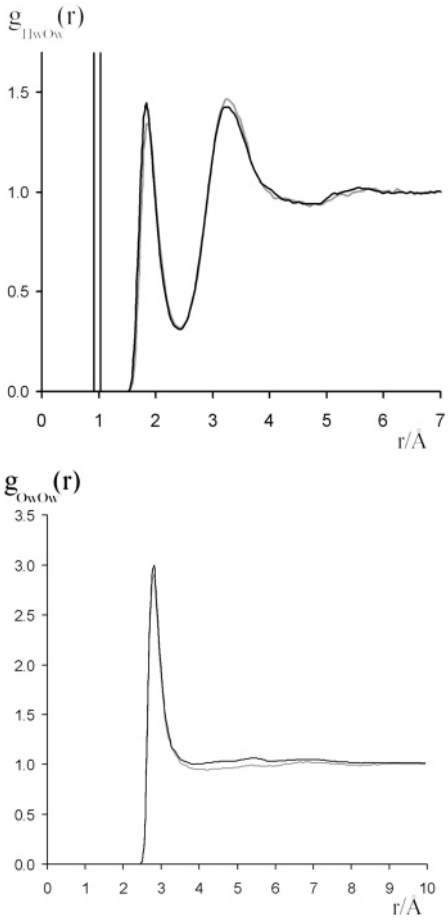

Figure 7. Upper: $g_{HwOw}(r)$'s calculated from MD simulation of 3.0 M* GdmSCN (gray line) and 1.5 M* Gdm_2SO_4 solution (black line). Lower: $g_{OwOw}(r)$, using the same colors for the two lines. Given that GdmSCN is a powerful denaturant, and Gdm_2SO_4 is not, the similarity in these functions as calculated from the MD simulations suggests that denaturant efficacy is not significantly dependent upon the water structure.

function and uses the component distributions calculated from the simulations to interpret the peaks in the experimental curves. All of the component distributions for the two solutions, as calculated from the MD simulations, are shown in Figure 8. While other pair correlations contributing to this composite function show ion pairing more clearly (i.e., $g_{NS}(r)$ and $g_{NGdmNthio}(r)$ for the guanidinium sulfate and guanidinium thiocyanate solutions, respectively, shown in Figure 9), these have insignificant weighting in the function ${}^nG_Y{}^Y(r)$ (eq 6). There are several intramolecular correlations below 2.5 Å, which are resolution-limited in the NDIS measurement. By far the most interesting features are the peaks at 3.7 and 4.9 Å, which are not resolution-limited. In both cases these are due to solvation of the Gdm^+ ion (Figure 6). The similarity between the NDIS and MD results, specifically with respect to the features that are directly related to the hetro-ion-pairing, shows that the MD reproduces the most important aspect of these systems (the ion−ion interactions). All of these peaks are due to the O−C and O−N correlations from oxygen atoms hydrogen-bonded to the Gdm^+ ion. In the Gdm_2SO_4 case these are mostly due to the oxygen atoms of the strongly associated sulfate ions, while in the thiocyanate case these are mostly due to oxygens of water molecules (Figure 10). The stronger association of the sulfate ion to Gdm^+ (than waters to Gdm^+ in the GdmSCN solution) is manifested in the NDIS data by more pronounced peaks at 3.7 and 4.9 Å (compare curves "c" in Figure 6). The relationship between the strong ion pairing observed in the MD simulation and peaks in the function ${}^nG_Y{}^Y(r)$ can be emphasized by examining only the $N_{Gdm}O$ component of this structure factor (Figure 10) which accounts for ∼30% of the function ${}^nG_Y{}^Y(r)$. In the GdmSCN solution this $N_{Gdm}O$ component is entirely due to oxygen atoms on water and exhibits peaks at 2.9 and 4.9 Å with a broad weak peak at 3.7 Å. In the Gdm_2SO_4 solution all three of these peaks are significantly more pronounced, and if the $N_{Gdm}O$ correlation is further broken down into correlations to oxygens on water (O_w) and oxygens on sulfate (O_{sulf}) as is shown in Figure 10, it is found that these enhanced features are almost exclusively due to O_{sulf}. These radial distribution functions also demonstrate the result observed from the density maps (Figure 2), that there is a significant preference for O_{sulf} to interact with the Gdm^+ over O_w. This is particularly clear here, as only 10% of the oxygen atoms in the Gdm_2SO_4 system are O_{sulf}, yet they account for more than 50% of the oxygens

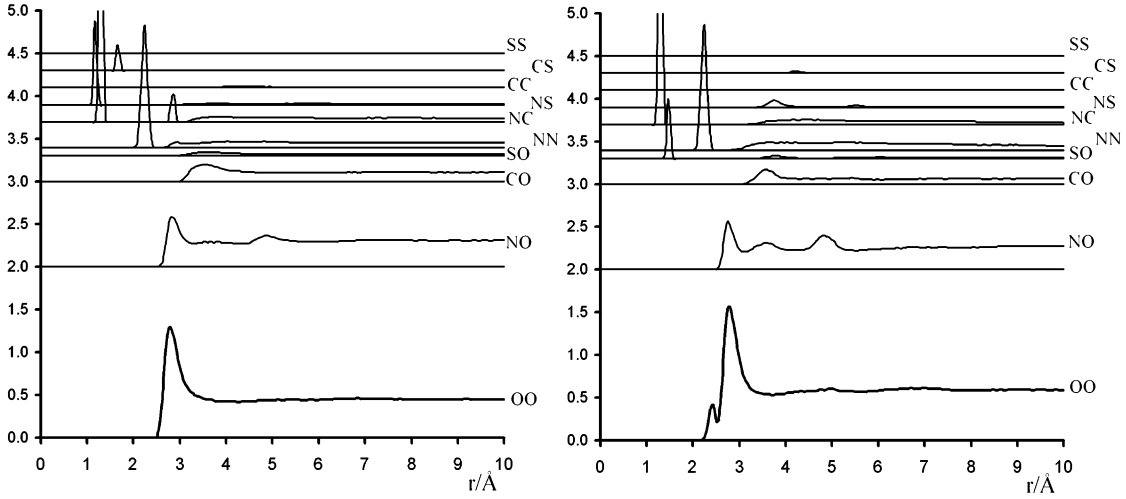

Figure 8. Individual component distribution functions for ${}^{n}G_{Y}^{Y}(r)$ for both solutions as calculated from MD simulations. The thiocyanate solution is shown on the left, and the sulfate solution is shown on the right.

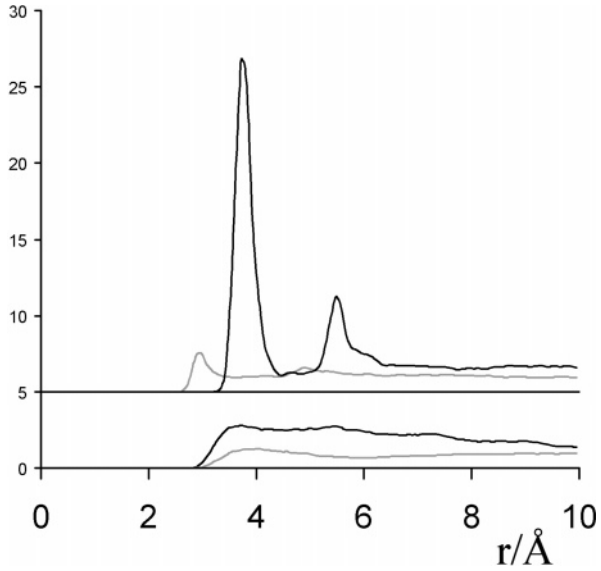

Figure 9. Upper are shown some of the $g(r)$'s that represent homo and hetero-ion pairing in the GdmSCN and Gdm_2SO_4 solution as calculated from MD simulations. Upper black is $g_{NS}(r)$ for the Gdm_2SO_4 and upper gray $g_{NGdmNthio}(r)$, where N_{thio} is the nitrogen atoms upon the thiocyanate ion. Clearly the $SO_4^{2-}-Gdm^+$ ion pairing is much stronger than the SCN^--Gdm^+ ion pairing. Lower is shown $g_{CC}(r)$ (the Gdm^+ homo-ion pairing), black for the SO_4^{2-} solution, and gray for the SCN^- solution. $g_{CGdmCGdm}(r)$ for the GdmSCN solution is very similar to that found in GdmCl solution and has a peak at 4.0 Å. However, for the Gdm_2SO_4 solution it is found that there is a general augmentation of Gdm^+ ions around a Gdm^+ ion up to a distance of about 1 nm.

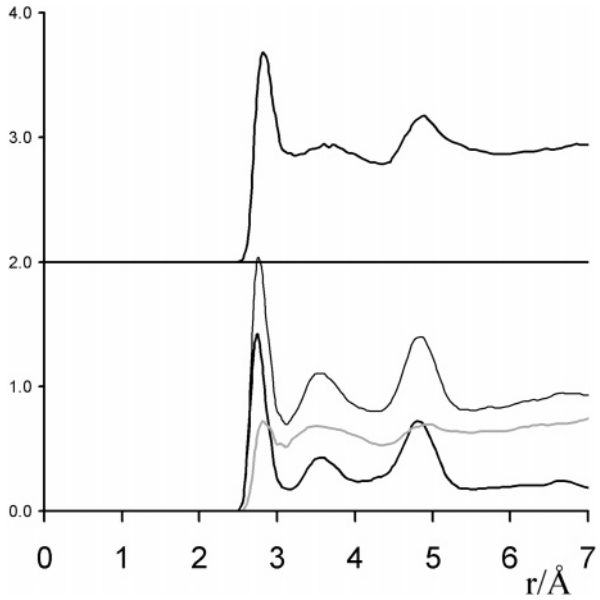

Figure 10. Upper: the function $g_{NGdmO}(r)$ for the GdmSCN solution. Lower: $g_{NGdmO}(r)$ for the Gdm_2SO_4 solution (uppermost thin black line). This has been subdivided into the contributions of this function from O_w (gray line) and O_{sulf} (bottom thick black line). The key observation is that although the O_{sulf} only constitutes 10% of the function $g_{NGdmO}(r)$, it actually contains almost all the structure observed in the function $g_{NGdmO}(r)$.

next to the Gdm^+ ion. In the GdmSCN solution the Gdm^+ ions form an average of 4.9 H bonds to water, while in the Gdm_2SO_4 solution it forms an average of only 2.7 H bonds to O_{wat} and 3.3 H bonds to O_{sulf}. While other radial distribution functions such as $g_{NS}(r)$ for the Gdm_2SO_4 solution demonstrate hetero-ion pairing much more strongly than $g_{NGdmO}(r)$ (Figure 9), they do not contribute significantly to the experimentally determinable function ${}^{n}G_{Y}^{Y}(r)$. This observation clearly demonstrates the occurrence of strong ion pairing in solution.

From the potential of mean force calculated from the $g_{CS}(r)$, the pairing free energy for Gdm^+ and SO_4^{2-} ions is estimated to be approximately $4kT$, which is roughly 4 times the pair formation energy between two water molecules in bulk water. This strong ion pairing between Gdm^+ and SO_4^{2-} is consistent with previous thermodynamic studies of sulfate ion binding by guanidinium-based anion chelators in solution[27] and in crystals[28] and is the underlying cause of the observed mesoscopic ion structuring. Previous potential of mean force calculations of Gdm^+ ion pairing in water did not address these effects of counterions[2,29] as these species were omitted from the simulations.

The direct examination of the experimental structure factor difference data shown in Figure 4 demonstrates that the strong ion pairing observed in the *r*-space data is not an artifact of the FT process but is clearly and directly observable in the experimental measurement. It should be noted that this difference function constitutes only about 10% of the total coherent scattering from a D_2O solution of these electrolytes. Further, the difference between strong and weak ion pairing is only a few percent in this difference function. Because of the exceptional stability of the D4C diffractometer,[30] the measurement

of this tiny difference is simple. However, this observation does emphasize the fact that stability is crucial in measuring structure by neutron diffraction of solutions and that instruments with lower stability (such as the SANDALS diffractometer at the Rutherford-Appleton Laboratory, which has a current quoted stability of ca. 1%) probably could not distinguish the different ion structuring in these solutions.

The lower the Q value of a feature, the larger the feature to which it corresponds in r-space. Most notably there is a peak in the residue from ${}^{n}\Delta_{Y}{}^{Y}(Q)$ of the Gdm_2SO_4 and GdmSCN solutions shown in Figure 4 at ca. 1 $Å^{-1}$ in the MD data that does not occur in the NDIS data. The interpretation of these data is uncertain; however, the NDIS data suggest that longer range (nanometer scale) structures exist in the Gdm_2SO_4 solution that do not occur in the GdmSCN solution. The logical extension of the demonstration of strong ion pairing is that longer range structures may exist. However, for this to be demonstrated clearly, good small-angle neutron scattering data are required. Such an experiment has been scheduled for Gdm_2SO_4. The suggestion of the presence of ionic aggregates in Gdm_2SO_4 would imply that such aggregates might be even more likely to form in guanidinium carbonate solutions due to the larger charge density on the carbonate oxygen atoms and the similar geometric features of this anion. Accordingly, on the basis of these results, a second set of MD and NDIS studies of guanidinium carbonate were designed to look for such aggregates. These studies produced even stronger diffraction signals resulting from heteroionic clustering. Subsequent SANS experiments on aqueous guanidinium carbonate conclusively demonstrated the presence of aggregates on the nanometer size scale.[31]

Conclusion

The neutron diffraction data reported here suggest ion pairing of such strength that it leads to ion ordering in solution on the mesoscopic length scale for sulfate. The observation of nanometer-scale aggregates in Gdm_2SO_4 solutions was unexpected and somewhat surprising. However, a recent dielectric relaxation study of aqueous magnesium sulfate solutions also found heteroion pairing with possibly more extended ionic aggregates.[32] Mesoscopic aggregation of ions is not generally considered in theories of aqueous solutions and would be expected to have direct consequences for the thermodynamic and kinetic properties of the system, including viscosity, diffusion, and conductance. The inference of a role for ion−ion interactions in determining Hofmeister ordering from the simulations alone would be less convincing if it was not supported by the direct experimental measure of solution structure using NDIS.

In the present study it was found that in Gdm_2SO_4 solutions the ions aggregate so strongly as to separate out as a network making the Gdm^+ unavailable for protein binding. Conversely, in GdmSCN solutions, the ions are more randomly distributed but interact so as to leave the Gdm^+ faces free to bind to protein hydrophobic groups. This difference is primarily a function of the difference in valency and molecular topology of the anions, with the tetrahedral character of the sulfate ion easily promoting the development of bonded networks in much the same way that the tetrahedral structure of water promotes the development of hydrogen-bonded networks. Clearly the strength of this pairing also depends on the atomic partial charges of the ions and the degree of polarization, but the observation of aggregation in a system with significantly lower polarity suggests that the qualitative observation of aggregation is not sensitively dependent on charge distribution.

Guanidinium ions in GdmCl solution have previously been found to pair through hydrophobic-like stacking of their planar faces.[4] The Gdm^+ stacking suggests a means by which this ion promotes the solubility of nonpolar side chains (particularly those of the aromatic amino acids). Studies of amino acid interactions in proteins have shown a preference for the guanidinium group of arginine to make stacking interactions with aromatic amino acids (especially tryptophan[33]), with the guanidinium nitrogen atoms around 3.6−3.8 Å from the aromatic rings.[34−36] The faces of the guanidinium cation (essentially a delocalized π system[37]) have hydrophobic properties that are likely to make the interaction with aromatic side chains favorable. Calculations have previously indicated that hydrated guanidinium cations can associate in a parallel orientation,[2−4] similar to that observed here. Thus, the enhanced solubilization of (aromatic) hydrophobic amino acid side chains would involve stacking with guanidinium ions (with the entropically favorable release into the bulk solution of water "ordered" by the hydrophobic group), while the denaturant ions are solvated by hydrogen bonding with water in the molecular plane as observed here. Again, precedents have been found in protein crystal structures in which arginine side chains that participate in aromatic stacking interactions often make hydrogen bond interactions in the molecular plane with either protein carbonyl groups[34,38] or water molecules.[39]

These experiments represent the most direct structural evidence of which we are aware to date of strong ion pairing at moderate concentration. Previous examples of such pairing[40] have been at such high concentration (∼20 m) that pairing is topologically inevitable. The ion pairing described here is so strong in the case of the guanidinium sulfate that it results in a previously unobserved mesoscopic structuring on the nanometer scale. This difference in behavior could explain the curious fact that sulfate reverses the denaturing effect of guanidinium and the Hofmeister ordering of these anions. From these results one can predict that the mesoscopic scale structure in the guanidinium sulfate solution would produce a characteristic peak in the small-angle neutron scattering (SANS). Experiments to test this hypothesis are planned.

Acknowledgment. We thank A. C. Barnes, G. Cuello, J. E. Enderby, and M.-L. Saboungi for helpful discussions and the anonymous reviewers of an earlier version of this paper for helpful comments. This project was supported by a grant from the National Institutes of Health (GM63018).

Supporting Information Available: Short movies depicting the initial configuration for both the thiocyanate and sulfate simulations as well as representative snapshots from later in the simulation. This material is available free of charge via the Internet at http://pubs.acs.org.

References and Notes

(1) Friedman, H. L.; Krishnan, C. V. In *Water: A Comprehensive Treatise*; Franks, F., Ed.; Plenum Press: New York, 1973; Vol. 3, pp 1−118.

(2) Boudon, S.; Wipff, G.; Maigret, B. *J. Phys. Chem.* **1990**, *94*, 6056−6061.

(3) No, K. T.; Nam, K.-Y.; Scheraga, H. A. *J. Am. Chem. Soc.* **1997**, *119*, 12917−12922.

(4) Mason, P. E.; Neilson, G. W.; Enderby, J. E.; Saboungi, M.-L.; Dempsey, C. E.; MacKerell, A. D.; Brady, J. W. *J. Am. Chem. Soc.* **2004**, *126*, 11462−11470.

(5) Hofmeister, F. *Arch. Exp. Pathol. Pharmakol.* **1888**, *24*, 247−260.

(6) Breslow, R.; Guo, T. *Proc. Natl. Acad. Sci. U.S.A.* **1990**, *87*, 167−169.

(7) Mason, P. E.; Neilson, G. W.; Barnes, A. C.; Enderby, J. E.; Brady, J. W.; Saboungi, M.-L. *J. Chem. Phys.* **2003**, *119*, 3347−3353.

(8) Omta, A. W.; Kropman, M. F.; Woutersen, S.; Bakker, H. J. *Science* **2003**, *301*, 347−349.

(9) Sidhu, K. S.; Goodfellow, J. M.; Turner, J. Z. *J. Chem. Phys.* **1999**, *110*, 7943−7950.
(10) Schmidt, R. K.; Karplus, M.; Brady, J. W. *J. Am. Chem. Soc.* **1996**, *118*, 541−546.
(11) Liu, Q.; Brady, J. W. *J. Am. Chem. Soc.* **1996**, *118*, 12276−12286.
(12) Soper, A. K.; Luzar, A. *J. Phys. Chem.* **1996**, *100*, 1357−1367.
(13) Brooks, B. R.; Bruccoleri, R. E.; Olafson, B. D.; Swaminathan, S.; Karplus, M. *J. Comput. Chem.* **1983**, *4*, 187−217.
(14) Jorgensen, W. L.; Chandrasekhar, J.; Madura, J. D.; Impey, R. W.; Klein, M. L. *J. Chem. Phys.* **1983**, *79*, 926−935.
(15) Neria, E.; Fischer, S.; Karplus, M. *J. Chem. Phys.* **1996**, *105*, 1902−1919.
(16) Sansone, R.; Ebner, C.; Probst, M. *J. Mol. Liq.* **2000**, *88*, 129−150.
(17) Cannon, W. R.; Pettitt, B. M.; McCammon, J. A. *J. Phys. Chem.* **1994**, *98*, 6225−6230.
(18) Dixit, S.; Crain, J.; Poon, W. C. K.; Finney, J. L.; Soper, A. K. *Nature (London)* **2002**, *416*, 829−832.
(19) Wallqvist, A. *J. Phys. Chem.* **1991**, *95*, 8921−8927.
(20) Raschke, T. M.; Tsai, J.; Levitt, M. *Proc. Natl. Acad. Sci. U.S.A.* **2001**, *98*, 5965−5969.
(21) Patra, M.; Karttunen, M. *J. Comput. Chem.* **2004**, *25*, 678−689.
(22) Berendsen, H. J. C.; Grigera, J. R.; Straatsma, T. P. *J. Phys. Chem.* **1987**, *91*, 6269−6271.
(23) Jeffrey, G. A. *An Introduction to Hydrogen Bonding*; Oxford University Press: Oxford, 1997.
(24) Mason, P. E.; Neilson, G. W.; Dempsey, C. E.; Barnes, A. C.; Cruickshank, J. M. *Proc. Natl. Acad. Sci. U.S.A.* **2003**, *100*, 4557−4561.
(25) Tsai, J.; Gerstein, M.; Levitt, M. *J. Chem. Phys.* **1996**, *104*, 9417−9430.
(26) Leberman, R.; Soper, A. K. *Nature (London)* **1995**, *378*, 364−366.
(27) Schmidtchen, F. P.; Berger, M. *Chem. Rev.* **1997**, *97*, 1609−1646.
(28) Hutchings, M. G.; Grossel, M. C.; Merckel, D. A. S.; Chippendale, A. M.; Kenworthy, M.; McGeorge, G. *Cryst. Growth Des.* **2001**, *1*, 339−342.
(29) Soetens, J.-C.; Millot, C.; Chipot, C.; Jansen, G.; Ángyán, J. G.; Maigret, B. *J. Phys. Chem. B* **1997**, *101*, 10910−10917.
(30) Fischer, H. E.; Palleau, P.; Feltin, D. *Physica B* **2000**, *276&278*, 93−94.
(31) Mason, P. E.; Kline, S. R.; Neilson, G. W.; Brady, J. W., unpublished results.
(32) Buchner, R.; Chen, T.; Hefter, H. G. *J. Phys. Chem. B* **2004**, *108*, 2365−2375.
(33) Gallivan, J. P.; Dougherty, D. A. *Proc. Natl. Acad. Sci. U.S.A.* **1999**, *96*, 9459−9464.
(34) Singh, J.; Thornton, J. M. *J. Mol. Biol.* **1990**, *211*, 595−611.
(35) Brocchieri, L.; Karlin, S. *Proc. Natl. Acad. Sci. U.S.A.* **1994**, *91*, 9297−9301.
(36) Flocco, M. M.; Mowbray, S. L. *J. Mol. Biol.* **1994**, *235*, 709−717.
(37) Ma, J. C.; Dougherty, D. A. *Chem. Rev.* **1997**, *97*, 1303−1324.
(38) Nandi, C. L.; Singh, J.; Thornton, J. M. *Protein Eng.* **1993**, *6*, 247−259.
(39) Thanki, N.; Thornton, J. M.; Goodfellow, J. M. *J. Mol. Biol.* **1988**, *202*, 637−657.
(40) Bertagnolli, H.; Zweier, H.; Mager, T. *J. Mol. Liq.* **1997**, *73*, *74*, 119−132.
(41) Humphrey, W.; Dalke, A.; Schulten, K. *J. Mol. Graphics* **1996**, *14*, 33−38.